JACS
JOURNAL OF THE AMERICAN CHEMICAL SOCIETY

Subscriber access provided by ISTANBUL TEKNIK UNIV

Article

Budding and Asymmetric Protein Microcompartmentation in Giant Vesicles Containing Two Aqueous Phases

M. Scott Long, Ann-Sofie Cans, and Christine D. Keating

J. Am. Chem. Soc., **2008**, 130 (2), 756-762 • DOI: 10.1021/ja077439c

Downloaded from http://pubs.acs.org on February 8, 2009

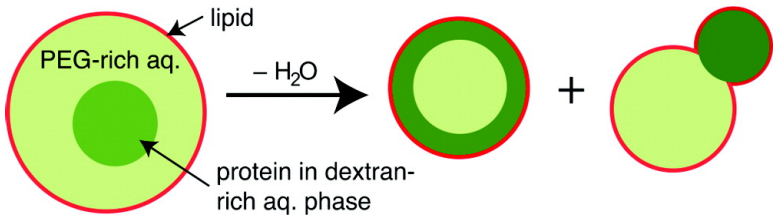

More About This Article

Additional resources and features associated with this article are available within the HTML version:

- Supporting Information
- Links to the 3 articles that cite this article, as of the time of this article download
- Access to high resolution figures
- Links to articles and content related to this article
- Copyright permission to reproduce figures and/or text from this article

View the Full Text HTML

ACS Publications
High quality. High impact.

Journal of the American Chemical Society is published by the American Chemical Society. 1155 Sixteenth Street N.W., Washington, DC 20036

J|A|C|S
ARTICLES
Published on Web 12/20/2007

Budding and Asymmetric Protein Microcompartmentation in Giant Vesicles Containing Two Aqueous Phases

M. Scott Long, Ann-Sofie Cans, and Christine D. Keating*

Department of Chemistry, The Pennsylvania State University, University Park, Pennsylvania 16802

Received September 26, 2007; E-mail: keating@chem.psu.edu

Abstract: We report the effect of external osmolarity on giant lipid vesicles containing an aqueous two-phase system (ATPS GVs). The ATPS, which is comprised of poly(ethyleneglycol) [PEG], dextran, and water, serves as a primitive model of the macromolecularly crowded environment of the cytoplasm. Coexisting PEG-rich and dextran-rich aqueous phases provide chemically dissimilar microenvironments, enabling local differences in protein concentration to be maintained within single ATPS GVs. The degree of biomolecule microcompartmentation can be increased by exposing the ATPS GVs to a hypertonic external solution, which draws water out of the vesicles, concentrating the polymers. Enrichment of a protein, soybean agglutinin, in the dextran-rich phase improves from 2.3-fold to 10-fold with an increase in external osmolarity from 100 to 200 mmol/kg. In some cases, budding occurs, with the bud(s) formed by partial expulsion of one of the two polymer-rich aqueous phases. Budding results in asymmetry in the internal polymer and biomolecule composition, giving rise to polarity in these primitive model cells. Budding is observed with increasing frequency as external ionic strength increases, when membrane elasticity permits, and can be reversed by decreasing external osmolarity. We note that the random symmetry-breaking induced by simple osmotic shrinkage resulted in polarity in both the structure and internal protein distribution in these primitive model cells. Budding in ATPS-containing GVs thus offers an experimental model system for investigating the effects of biochemical asymmetry on the length scale of single cells.

Introduction

Experimental models of biological cells are of interest for testing hypotheses on the properties and functional significance of various cellular structures (e.g., the lipid membrane) and as possible routes to understanding and/or duplicating the earliest cells.[1−4] We have been developing a model cell in which the macromolecularly crowded cytoplasmic interior[5] is mimicked by an aqueous solution of poly(ethyleneglycol) [PEG] and dextran polymers.[6,7] Aqueous solutions above a few weight percent of these polymers phase separate into coexisting PEG-rich and a dextran-rich aqueous phases.[8−10] Partitioning between these phases provides a route to reversible microcompartmentation[11−12] of biomolecules such as proteins and nucleic acids within the aqueous interior of our synthetic cells. Here we discuss the effect of osmotic stress on these aqueous two-phase system (ATPS)[8−10]-containing giant vesicles (GV)[1,13,14] and introduce model cells in which a protein is asymmetrically distributed within the model cytoplasm.

The response to external osmotic pressure has been studied for conventional GVs that lack an ATPS. Surprisingly, GV shrinkage under osmotic stress does not generally result in vesicle deflation. Instead, GVs retain their spherical shape after shrinkage. Helfrich and co-workers observed shape fluctuations during the process, followed by spherical morphologies. These authors proposed that submicroscopic daughter vesicles were reducing the GV surface area.[15] Similar repeating transitions from fluctuating to spherical GVs were observed by Umeda et al. upon addition of surfactant; this was interpreted as membrane

(1) Menger, F. M.; Angelova, M. I. *Acc. Chem. Res.* **1998**, *31*, 789−797.
(2) (a) Svetina, S.; Zeks, B. *Anatom. Rec., Part A* **2002**, *266*, 215−225. (b) Kiser, P.; Wilson, G.; Needham, D. *Nature* **1998**, *394*, 459−462. (c) Stauch, O.; Uhlmann, T.; Frohlich, M.; Thomann, R.; El-Badry, M.; Kim, Y.-K.; Schubert, R. *Biomacromolecules* **2002**, *3*, 324−332. (d) Karlsson, M.; Davidson, M.; Karlsson, R.; Jesorka, A.; Lobovkina, T.; Hurtig, J.; Voinova, M.; Orwar, O. *Annu. Rev. Phys. Chem.* **2004**, *55*, 613−649. (e) Cans, A.-S.; Wittenberg, N.; Karlsson, R.; Sombers, L.; Karlsson, M.; Orwar, O.; Ewing, A. *Proc. Natl. Acad. Sci. U.S.A.* **2003**, *100*, 400−404.
(3) (a) Forster, A. C.; Church, G. M. *Mol. Syst. Biol.* **2006**, *22*, 1−10. (b) Monnard, P.-A. *J. Membr. Biol.* **2003**, *191*, 87−97.
(4) (a) Noireaux, V.; Libchaber, A. *Proc. Natl. Acad. Sci. U.S.A.* **2004**, *101*, 17669−17674. (b) Chen, I. A.; Salehi-Ashtiani, K.; Szostak, J. A. *J. Am. Chem. Soc.* **2005**, *127*, 13213−13219. (c) Nomura, S.-i. M.; Yoshikawa, Y.; Yoshikawa, K.; Dannenmuller, O.; Chasserot-Golaz, S.; Ourisson, G.; Nakatani, Y. *ChemBioChem* **2001**, 457−459. (d) Nomura, S.-i. M.; Tsumoto, K.; Hamada, T.; Akiyoshi, K.; Nakatani, Y.; Yoshikawa, K. *ChemBioChem* **2003**, *4*, 1172−1175. (e) Fischer, A.; Franco, A.; Oberholzer, T. *ChemBioChem* **2002**, *3*, 409−417.
(5) (a) Zimmerman, S. B.; Minton, A. P. *Annu. Rev. Biophys. Biomol. Struct.* **1993**, *22*, 27−65. (b) Ellis, R. J. *Trends Biochem. Sci.* **2001**, *265*, 597−604.
(6) Long, M. S.; Jones, C. D.; Helfrich, M. R.; Mangeney-Slavin, L. K.; Keating, C. D. *Proc. Natl. Acad. Sci. U.S.A.* **2005**, *102*, 5920−5925.
(7) Helfrich, M. R.; Mangeney-Slavin, L. K.; Long, M. S.; Djoko, K. Y.; Keating, C. D. *J. Am. Chem. Soc.* **2002**, *124*, 13374−13375.
(8) Walter, H.; Johansson, G., Eds. *Methods Enzymol.* **1994**, *228*.
(9) Albertsson, P-Å. *Partition of Cell Particles and Macromolecules*, 3rd ed.; John Wiley and Sons: New York, 1986.
(10) Zaslavsky, B. Y. *Aqueous Two-Phase Partitioning: Physical Chemistry and Bioanalytical Applications*; M. Dekker: New York, 1995.
(11) Walter, H.; Brooks, D. E.; Srere, P. A. *Int. Rev. Cytol.* **2000**, *192*.
(12) Walter, H.; Brooks, D. E. *FEBS Lett.* **1995**, *361*, 135−139.
(13) Giant Vesicles. Luisi, P. L., Walde, P., Eds. In *Perspectives in Supramolecular Chemistry. vol. 6*; John Wiley and Sons: West Sussex, U.K., 2000.
(14) Dimova, R.; Aranda, S.; Bezlyepkina, N.; Nikolov, V.; Riske, K. A.; Lipowsky, R. *J. Phys.: Condens. Matter* **2006**, *18*, S1151−S1171.
(15) Boroske, E.; Elwenspoek, M.; Helfrich, W. *Biophys. J.* **1981**, *34*, 95−109.

10.1021/ja077439c CCC: $40.75 **© 2008 American Chemical Society**

Scheme 1. Structures Formed When ATPS-Containing GV, with PEGylated DOPE in Their Membranes, Are Exposed to Osmotic Stress by Addition of a Sucrose Solution of 2× Osmolarity

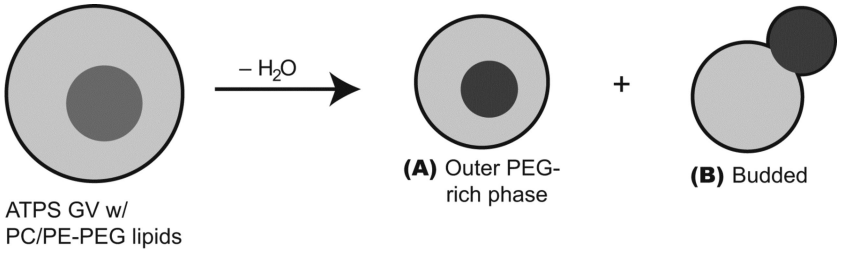

loss due to the surfactant but could also be consistent with osmotic shock due to the concentrated surfactant solution.[16] In some cases, osmotic pressure-induced, budded structures were large enough to have been imaged via optical microscopy.[17−19] For example, Meglio and co-workers reported the formation of raspberry-like structures in which small daughter vesicles budded into the GV interior upon carefully controlled osmotic stress.[17] Viallat et al. observed a wide variety of GV shapes after stepwise osmotic shrinkage, consistent with structures predicted by an area difference elasticity model.[19] These authors also examined osmotic shrinkage of GVs filled with an agarose gel, finding shapes not seen for gel-free vesicles, such as spikes and wrinkles.[19] Osmotically and sonication-induced morphological changes, including budding, have also been observed for block-copolymer vesicles.[20]

GV budding has been observed in the absence of osmotic stress, for example, when gel phase lipids are heated above the liquid/gel phase transition temperature to increase the surface area-to-volume ratio of the vesicles.[21] Optical radiation pressure[22] and decompression after high hydrostatic pressure treatment[23] have also been reported to cause budding in GVs. Additionally, when coexisting lipid phase domains are present in the membrane, budding is both expected and observed due to differences in the spontaneous curvature of the domains and the line tension at the domain boundaries.[24−29] Buds coincide with the lipid phase domains and, hence, have a different lipid composition than that of the rest of the vesicle. In all of the above examples, the *aqueous interior content* of the buds is the same as that for the body of the vesicle.

Here, we report the effect of osmotic stress on GVs containing coexisting aqueous phases (ATPS GVs). We observed three classes of ATPS GV morphologies upon osmotic dehydration: (A) spherical vesicles with the PEG-rich phase contacting the lipid membrane; (B) nonspherical vesicles in which one or more buds protrude from the central sphere, such that the buds contain one of the aqueous phases (e.g., dextran-rich) and the body of the vesicle contained the other (PEG-rich) aqueous phase; and (C) spherical vesicles with the dextran-rich phase contacting the lipid membrane (Schemes 1 and 2). For the ATPS compositions used here, the dextran-rich phase is generally smaller, such that when the two phases cease to be concentric, it appears as a "bud" on the larger PEG-rich phase. Which of these structures was observed in a given experiment depended on the degree of hypertonicity, the ATPS polymer composition, and the lipid membrane composition. Budding occurred with increasing frequency as the osmolarity of the ATPS GV dispersion and/or the deformability of the lipid membrane increased. This process could be reversed by decreasing external osmolarity, such that the protruding aqueous phase re-entered the vesicle as it returned to a spherical shape. The partitioning of both the dextran polymer itself and of proteins that were partitioned into the dextran-rich aqueous phase increased with increasing osmolarity. Importantly, budding in these ATPS GVs induced asymmetric distribution not only of the aqueous phases but also of the proteins preferentially partitioned to one of the aqueous phases.

Scheme 2. Structures Observed for ATPS GVs with DOPC/DOPC Membranes Lacking PEGylated Lipid

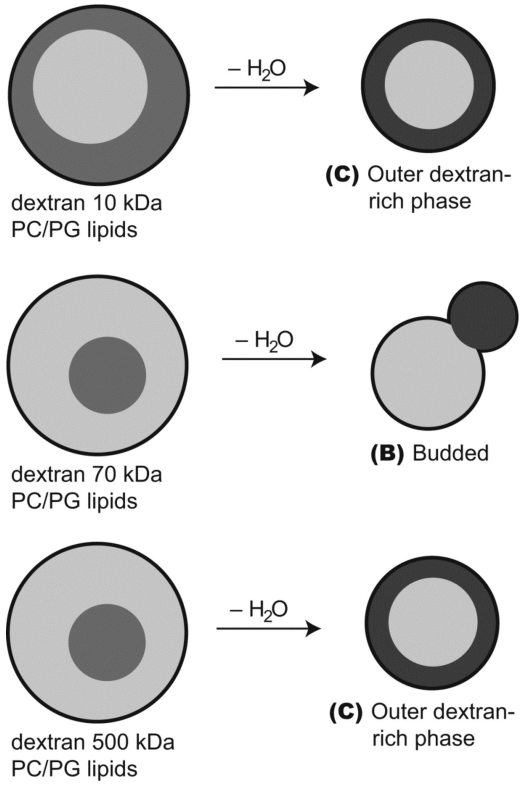

(16) Umeda, T.; Nomura, F.; Inaba, T.; Takiguchi, K.; Hotani, H. *ChemPhysChem* **2005**, *6*, 1047−1050.
(17) Bernard, A.-L.; Guedeau-Boudevile, M.-A.; Jullien, L.; di Meglio, J.-M. *Biochim. Biophy. Acta* **2002**, *1567*, 1−5.
(18) Menager, C.; Cabuil, V. *J. Phys. Chem. B* **2002**, *106*, 7913−7918.
(19) Viallat, A.; Dalous, J.; Abkarian, M. *Biophys. J.* **2004**, *86*, 2179−2187.
(20) (a) Zhou, Y.; Yan, D. *Angew. Chem., Int. Ed.* **2005**, *44*, 3223−3226. (b) Zhou, Y.; Yan, D. *J. Am. Chem. Soc.* **2005**, *127*, 10468−10469.
(21) (a) Dobereiner, H. G.; Kas, J.; Noppl, D.; Sprenger, I.; Sackmann, E. *Biophys. J.* **1993**, *65*, 1396−1403. (b) Kas, J.; Sackmann, E. *Biophys. J.* **1991**, *60*, 825−844.
(22) Kitamura, N.; Sekiguchi, N.; Kim, H.-B. *J. Am. Chem. Soc.* **1998**, *120*, 1942−1943.
(23) Beney, L.; Perrier-Cornet, J. M.; Hayert, M.; Gervais, P. *Biophys. J.* **1997**, *72*, 1258−1263.
(24) Baumgart, T.; Hess, S. T.; Webb, W. W. *Nature* **2003**, *425*, 821−824.
(25) Kumar, P. B. S.; Gompper, G.; Lipowsky, R. *Phys. Rev. Lett.* **2001**, *86*, 3911−3914.
(26) Sackmann, E.; Feder, T. *Mol. Membr. Biol.* **1995**, *12*, 21−28.
(27) Julicher, F.; Lipowsky, R. *Phys. Rev. E* **1996**, *53*, 2670−2683.
(28) Allain, J.-M.; Amar, M. B. *Eur. Phys. J. E* **2006**, *20*, 409−420.
(29) Li, L.; Liang, X.; Lin, M.; Qui, F.; Yang, Y. *J. Am. Chem. Soc.* **2005**, *127*, 17996−17997.

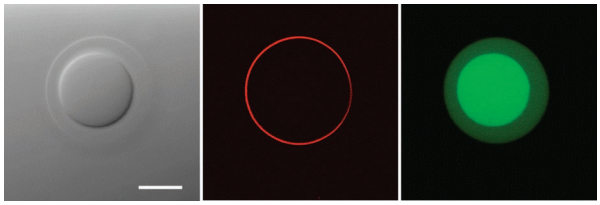

Figure 1. Confocal images of an ATPS-containing GV in isotonic PEG-rich external phase, imaged with transmitted light (left), rhodamine-DOPE fluorescence (middle), and Alexa488-dextran 10 kDa fluorescence (right). ATPS GV was prepared in a 7.5% 8 kDa PEG/8.0% 10 kDa dextran/5 mM sodium phosphate pH 7.0 ATPS, with lipid composition 44:1 mol ratio DOPC/DOPE-mPEG 2000). $T = 5$ °C. Scale bar = 5 microns.

Thus, the random symmetry-breaking induced by simple osmotic shrinkage resulted in polarity in both the structure and internal protein distribution in these primitive model cells. Not only are the resulting structures superficially similar to polar living cells such as budding yeast, but the lack of deterministic control over the direction of the bud(s) is reminiscent of recent hypotheses proposing a stochastic origin for polarity in living cells, followed by asymmetry amplification.[30,31]

Results and Discussion

ATPS GVs were formed by swelling a dried lipid film[32−34] in a warm polymer solution (the ATPS at 37 °C, above its phase transition temperature, where it is a single phase).[6,7] Upon cooling to 5 °C, phase separation occurred in both the vesicle interior and the bulk solution. ATPS GV imaging was facilitated by removal from the bulk ATPS interface and dispersing them in an isotonic solution that is a single phase. For this, we used the PEG-rich (i.e., top) phase of a bulk ATPS having the same polymer composition as that of the PEG-rich phase used to form the ATPS/GVs, minus the lipid and any fluorophore-tagged polymers or solutes. This avoided any inadvertent changes in osmotic pressure. Figure 1 shows transmitted and confocal fluorescence images for an ATPS GV suspended in this isotonic PEG-rich phase. Under these conditions, vesicles are generally spherical or spheroidal, with aqueous interiors composed of a dextran-rich phase surrounded by a PEG-rich phase.[6] In Figure 1 the dextran-rich phase has been stained with Alexa488-labeled dextran 10 kDa for visualization. The dextran-rich aqueous phase occupies the inner position, with the PEG-rich aqueous phase fully surrounding it and contacting the membrane. This is the geometry observed for all ATPS compositions tested, when our standard lipid membrane composition of 44:1 mol ratio DOPC/DOPE-mPEG 2000 Da was used. Except where otherwise noted, the following discussion focuses on ATPS GV with this lipid composition and with an aqueous polymer solution of 7.5 wt % PEG 8 kDa, 8.0 wt % dextran 10 kDa, 5 mM pH 7.0 phosphate buffer present during GV formation.

Effect of Hypertonic Sucrose on ATPS GV Morphology. When ATPS GVs were suspended in a hypertonic external solution, the vesicles shrank without becoming flaccid (similar to GVs without encapsulated ATPS),[15,17,18] and in many cases budding occurred, with one or more buds forming and remaining attached to the parent vesicle (Scheme 1). The protruding "buds" contained one of the aqueous phases, and the "body" contained the other. Figure 2 shows budded ATPS GVs prepared at an osmolarity of 113 mmol/kg and subsequently dispersed in a hypertonic sucrose solution (152 mmol/kg). The images in Figure 2 demonstrate the variety of morphologies observed within a single batch of vesicles. Some ATPS GVs did not form buds, while others formed one or several. The predominant morphology in these samples was singly budded ATPS GVs. We observed fission of the buds from the parent vesicle only rarely. The number of ATPS GVs having buds, as well as the number of buds per vesicle, increased as the osmolarity of the vesicle dispersion increased. ATPS GVs could be successfully dispersed in media of osmolality in excess of 800 mmol/kg. For comparison, *E. coli* bacteria can adjust to a much larger range of osmotic stress environments than those used in the ATPS GV experiments and can maintain growth over a 100-fold range in osmolarities.[35]

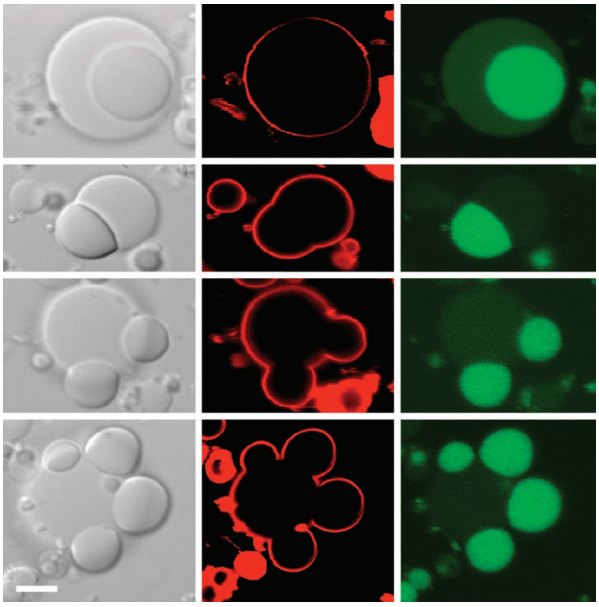

Figure 2. Confocal micrographs illustrating the response of 44:1 mol ratio DOPC/DOPE-mPEG 2000 Da ATPS GVs to osmotic stress. These ATPS GVs are dispersed in 152 ± 1.00 mmol/kg sucrose/buffer. Columns, from left: transmitted light (DIC), lipid fluorescence, lectin SBA fluorescence. $T = 5$ °C, bar = 10 μm.

Budding in ATPS GVs is fundamentally different from *lipid membrane* phase domain-driven budding in GVs that do not contain ATPS,[21,25−28,36,37] both in the mechanism of formation and in the organization of the interior aqueous compartment. The budded ATPS GV structures described here contain coexisting internal PEG-rich and dextran-rich aqueous phases, which provide microcompartments into which solutes can be localized. They do not exhibit any obvious domain formation in their lipid bilayers. For the vesicles in Figure 2, fluorophore-labeled soy bean agglutinin (SBA)[38] was localized in the dextran-rich phase via affinity for the dextran polymer. The

(30) Edlich-Soldner, R.; Li, R. *Nat. Cell Biol.* **2003**, *5*, 267−270.
(31) Harris, S. D. *Int. Rev. Cytol.* **2006**, *251*, 41−77.
(32) Yamashita, Y.; Oka, M.; Tanaka, T.; Yamazaki, M. *Biochim. Biophys. Acta* **2002**, *1561*, 129−134.
(33) Szleifer, I.; Gerasimov, O. V.; Thompson, D. H. *Proc. Natl. Acad. Sci. U.S.A.* **1998**, *95*, 1032−1037.
(34) Akashi, K.-I.; Miyata, H.; Itoh, H.; Kinosita, K., Jr. *Biophys. J.* **1996**, *71*, 3242−3250.
(35) Record, M. T., Jr.; Courtenay, E. S.; Cayley, D. S.; Guttman, H. J. *Trends Biochem. Sci.* **1998**, *23*, 143−148.
(36) Veatch, S. L.; Keller, S. L. *Biochim. Biophys. Acta* **2005**, *1746*, 172−185.
(37) Baumgart, T.; Hess, S. T.; Webb, W. W. *Nature* **2003**, *425*, 821−824.
(38) Lis, H.; Sharon, N. *Chem. Rev.* **1998**, *98*, 637−674.
(39) Dominak, L. M.; Keating, C. D. *Langmuir* **2007**, *23*, 7148−7154.
(40) Lasic, D. *Biochem. J.* **1988**, *256*, 1−11.
(41) Sriwongsitanont, S.; Ueno, M. *Colloid Polym. Sci.* **2004**, *282*, 753−760.

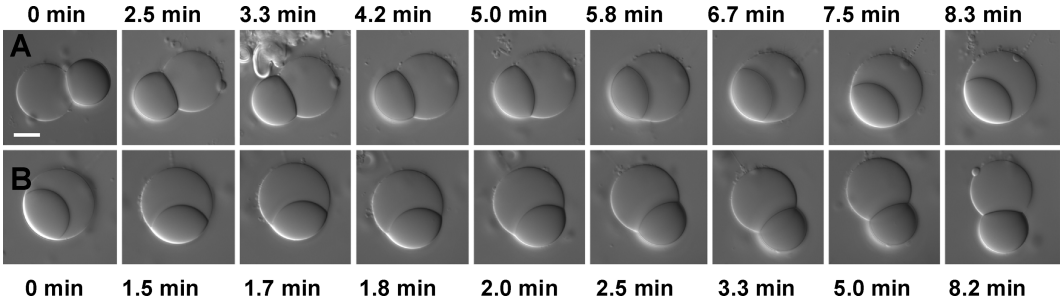

Figure 3. DIC images of dynamic aqueous phase budding within an ATPS GV. This ATPS GV (44:1 mol ratio DOPC/DOPE-mPEG 2000 Da) was originally imaged in a hypertonic sucrose/buffer solution. The times above (below) each frame are the minutes into the process that the images were acquired. (A) Transition induced by adding DI water. (B) Transition induced by adding hypertonic sucrose. $T = 3$ °C, bar = 10 μm.

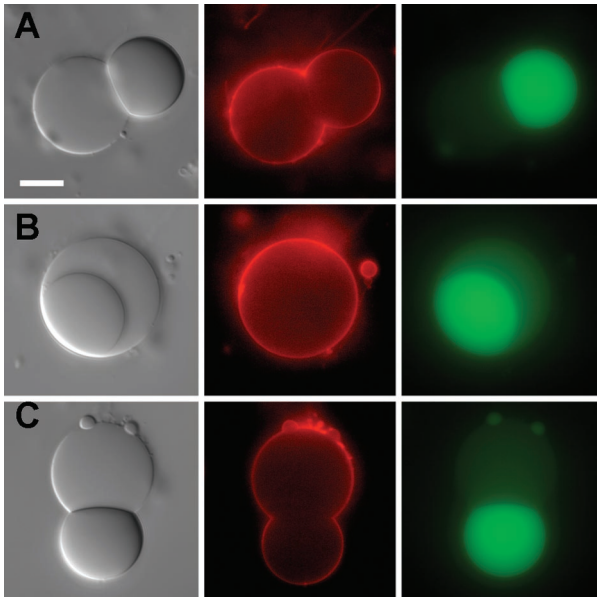

Figure 4. Micrographs of dynamic asymmetric protein microcompartmentation within an ATPS GV. This is the same vesicle as those in Figure 3. (A) Before dilution. (B) After dilution. (C) After concentration. Columns, from left: transmitted light (DIC), lipid fluorescence, lectin SBA fluorescence. $T = 3$ °C, scale bar = 10 μm.

dextran-rich buds had locally higher SBA concentrations as compared to the body of the vesicle. This is interesting because it provides a route to asymmetric chemical and biochemical distributions in our primitive model cells. The onset of polarity in single cells is a critical step in differentiation and morphogenesis; both the mechanism and consequences of cell polarity are only beginning to be understood.[30,31]

Budding in ATPS GVs was reversible. When the osmotic pressure of the external solution was reduced (from 200 to 100 mmol/kg, close to isotonic with the initial 113 mmol/kg at which the ATPS GVs had been prepared), "buds" moved back into the body of the vesicles, returning the ATPS GVs to a spherical morphology. A subsequent increase in the external sucrose concentration (to 200 mmol/kg) resulted in the reappearance of buds. Figures 3 and 4 and Supporting Information Figures 2 and 3 illustrate this process. The volume loss for this vesicle upon budding was ~20% of its initial volume at 113 mmol/kg (we have observed volume losses as high as 55% and as low as 15% for other vesicles exposed to the same changes in osmolality). Note that the ATPS GVs were freely suspended, and therefore both rotated and translated upon introduction of external solutions. The images in Figure 4 have been cropped

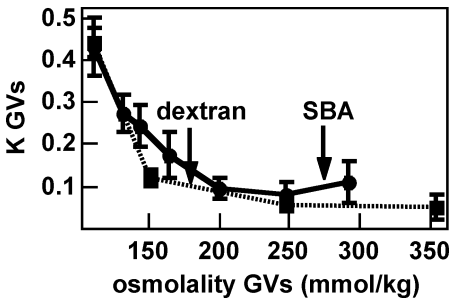

Figure 5. Partitioning of dextran 10,000 Da and lectin SBA in ATPS GVs (44:1 mol ratio DOPC/DOPE-mPEG 2000 Da) as a function of ATPS GV suspension osmolality. $T = 5$ °C. At least 40 ATPS GVs were measured for each data point.

to center the vesicle; however rotations were left as observed. Since SBA remained concentrated in the dextran-rich phase, the asymmetric protein microcompartmentation generated by budding was also reversible in these experiments. We note that it is possible to convert the GV interior to a single aqueous phase by exposure to a hypotonic solution, resulting in homogeneous polymer and protein distribution inside the GV.[6]

Increased Protein Partitioning. Osmotic shrinkage concentrates both polymers of the ATPS within the GVs. This should result in increased partitioning of both the PEG and dextran polymers and any solutes in the ATPS.[8,9] Partitioning is quantified by the partition coefficient, K, which is equal to the concentration of a solute in the PEG-rich phase divided by its concentration in the dextran-rich phase. Thus, fractional K values indicate a preference for the dextran-rich phase. Figure 5 shows the effect of external osmolality on SBA and dextran partitioning in ATPS GVs, as determined from confocal fluorescence microscopy. SBA partitioning improves from a K of ~0.44 to ~0.1 (an improvement from a 2.3× to 10× higher protein concentration in the dextran-rich phase as compared with the PEG-rich phase) with an increase in external osmolarity from 100 to 200 mmol/kg. Although partitioning within ATPS GVs was always lower than that for the corresponding bulk solutions,[6] the general trend of increasing both polymer and solute partitioning with increasing polymer weight percent composition was qualitatively analogous to experiments in a bulk ATPS in which the weight percent ratio of the polymers was held constant while increasing the total polymer weight percent (Supporting Information Figures 4 and 5).[6] ATPS composition, and consequently K, varies between vesicles within a batch due to differences in polymer encapsulation efficiencies.[6,39] Histograms for SBA partitioning within ATPS GVs as a function of osmolarity are shown in Supporting Information Figure 6.

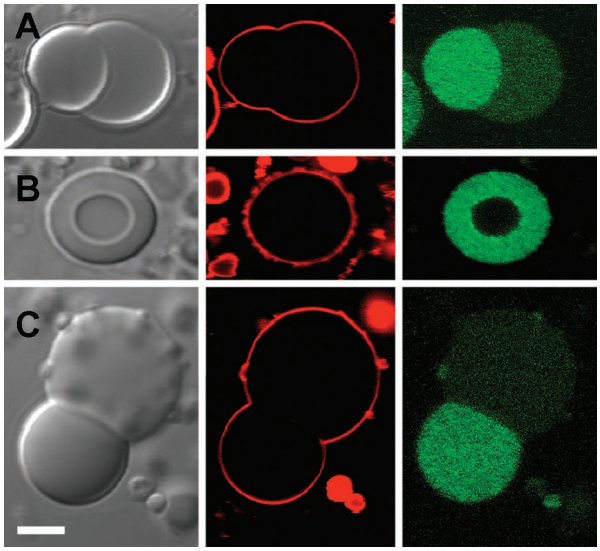

Figure 6. Confocal micrographs illustrating the differential effects of osmotic stress on ATPS GV morphology as a function of the lipids in the GV membrane. (A) 44:1 mol ratio DOPC/DOPE-mPEG 2000 Da GV, dispersed in 133 ± 2.08 mmol/kg sucrose/buffer; (B) 10:1 mol ratio DOPC/DOPG GV, dispersed in 816 ± 3.00 mmol/kg sucrose/buffer; (C) 44:10:1 mol ratio DOPC/DOPG/DOPE-mPEG 2000 Da GV, dispersed in 289 ± 1.00 mmol/kg sucrose/buffer. Note that these osmolalities were arbitrarily chosen for the figure. Columns, from left: transmitted light (DIC), lipid fluorescence, lectin SBA fluorescence. $T = 5$ °C, bar = 10 μm.

Effect of Lipid Composition. Exposure to hypertonic sucrose solutions can result not only in budded vesicles, with both aqueous phases contacting the lipid membrane, but also in smaller spherical vesicles with either the PEG- or dextran-rich aqueous phase contacting the membrane. The observed morphologies depend in part on lipid composition. Figure 6 shows typical morphologies for PEG 8 kDa/dextran 10 kDa ATPS GVs prepared with DOPC as the primary lipid component, and with smaller amounts added of either PEGylated DOPE or DOPG, or both. Lipids with PEGylated or charged headgroups (e.g., DOPG) are often used in GV preparations to assist separation of the lamella during GV formation.[40−42] ATPS GVs with membranes containing a PEGylated lipid bud in hypertonic sucrose solutions (Figure 6A and C). DOPC/DOPG liposomes do not generally bud under these conditions but instead remain spherical with the dextran-rich phase in contact with the lipid membrane (Figure 6B). The ATPS GV shown in Figure 6B did not bud even when exposed to a much higher osmotic pressure than that needed to induce budding in ATPS GVs when PEG-modified membranes were present (816 mmol/kg as compared with 133 and 289 mmol/kg).

Incorporation of PEG-grafted lipids alters membrane bending elasticity,[43,44] which facilitates the deformation required for budding. Figure 7 shows the effect of PEGylated DOPE in the lipid membranes of PEG 8kDa/dextran 10 kDa ATPS GVs in a hypertonic solution. DOPG was also included in these vesicle preparations to facilitate ATPS GV formation, which is otherwise challenging at low PEG-DOPE lipid concentrations. The percent of budded GV in the preparation increased from <10% initially to >60% at just 2 mol % PEGylated lipid. Polymer-grafted lipids such as the DOPE-PEG 2000 used here undergo a mushroom-to-brush transition as their mole fraction in the lipid membrane increases. At very low densities, individual polymer chains are separated from each other, resulting in a mushroom-like morphology. As the mole fraction is increased, the polymer chains begin to interact and extend from the surface to give a uniform, brushlike coating. For PEG 2000, which has 45 oxyethylene repeats and a Flory radius of 3.8 nm, the mushroom-to-brush transition is expected at the 1.4% PEGylated lipid.[45] Thus, the data in Figure 7 suggest increased budding up to the mushroom-to-brush transition, after which the amount of budding stays essentially constant.

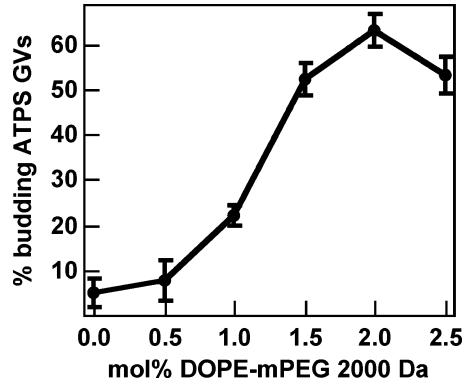

Figure 7. Percentage of budding, relative to concentric, ATPS GVs within a given preparation of DOPC/DOPG/DOPE-mPEG 2000 Da GVs. The mol ratio of DOPC/DOPG was held constant at 10:1, while the mol % of DOPE-mPEG 2000 Da was varied. These ATPS GVs were dispersed in 562 ± 1.53 mmol/kg sucrose/buffer prior to imaging. $T = 25$ °C. Between 20 and 41 ATPS GVs were measured for each data point.

Other factors that affect membrane deformability also impact the occurrence of budding in ATPS GVs. For example, cholesterol is known to increase membrane stiffness, with bending moduli increasing several-fold for cholesterol-saturated vs cholesterol-free SOPC membranes.[14,46] Addition of 40% cholesterol to the 2% PEGylated membranes resulted in a 2−3-fold reduction in ATPS GV budding. Heating, which can result in an increased membrane surface area,[47] can also favor budding. ATPS GVs prepared with 9:1 POPC:POPG membranes encapsulating a 3.75% PEG 8 kDa/4.5% dextran 482 kDa ATPS remained spherical in hypertonic sucrose. Upon heating to 50 °C, approximately half of the ATPS GVs budded.[7]

Effect of ATPS Polymer Composition. ATPS-containing GVs generally form as spheres with an inner polymer-rich phase surrounded by an outer polymer-rich phase that contacts the membrane. This morphology eliminates contact between the innermost aqueous phase and the membrane and minimizes the contact area between the two aqueous phases, while maintaining a spherical geometry. Budding can be understood as the minimization of the ATPS interfacial area under conditions where membrane deformability permits a nonspherical geometry.

Table 1 compares the aqueous−aqueous interfacial tensions and relative phase positions for four different ATPS composi-

(42) Navas, B. P.; Loner, K.; Deutsch, G.; Sevcsik, E.; Riske, K. A.; Dimova, R.; Garidel, P.; Pabst, G. *Biochim. Biophys. Acta* **2005**, *1716*, 40−48.
(43) Evans, E.; Heinrich, V.; Ludwig, F.; Rawicz, W. *Biophys. J.* **2003**, *85*, 2342−2350.
(44) Marsh, D. *Biophys. J.* **2001**, *81*, 2154−2162.
(45) Marsh, D.; Bartucci, R.; Sportelli, L. *Biochim. Biophys. Acta* **2003**, *1615*, 33−59.
(46) Song, J.; Waugh, R. E. *Biophys. J.* **1993**, *64*, 1967−1970.
(47) Kwok, R.; Evans, E. *Biophys. J.* **1981**, *35*, 637−652.
(48) Vonnegut, B. *Rev. Sci. Instrum.* **1942**, *13*, 6−9.
(49) Princen, H. M.; Zia, I. Y. Z.; Mason, S. G. *J. Colloid Interface Sci.* **1967**, *23*, 99−107.
(50) Helfrich, M. R.; El-Kouedi, M.; Etherton, M. R.; Keating, C. D. *Langmuir* **2005**, *21*, 8478−8486.

Table 1. Interfacial Tensions and Phase Position as a Function of ATPS and Membrane Composition

ATPS (w/w%)	interfacial tension ($\times 10^{-3}$ dyn/cm)[a]	outer phase PG/PC lipid isotonic[b]	outer phase PG/PC lipid hypertonic[c]	outer phase PEG-lipid isotonic[d]
9.4% PEG 4.6 kDa 9.4% dextran 10 kDa	5.2 ± 0.7	dextran	dextran	PEG
7.5% PEG 8 kDa 8.0% dextran 10 kDa	3.5 ± 0.9	dextran	dextran	PEG
5.3% PEG 8 kDa 4.0% dextran 70 kDa	0.4 ± 0.3	PEG	budded	PEG
4.1% PEG 8 kDa 2.6% dextran 500 kDa	0.5 ± 0.1	PEG	dextran	PEG

[a] Mean from two or three separate ATPSs. [b] External solution is top (PEG) phase of the ATPS used to form the GVs. [c] External solution is sucrose at 2× higher osmolarity than the ATPS used to form the GVs. [d] Hypertonic not shown since all GVs with PEGylated lipids budded in hypertonic solution.

tions. Polymer weight percents for each ATPS were selected for encapsulation based on their bulk phase behavior (i.e., such that the solution existed as two phases at our imaging temperature (generally 5 °C) and as a single phase at the GV preparation temperature (generally 37 °C)). Schemes 1 and 2 illustrate the morphologies observed upon exposure of as-prepared ATPS-GVs to hypertonic sucrose solutions; the conditions under which each of these morphologies is observed are given in Table 1. For all of the ATPS compositions encapsulated in vesicles with 2 mol % PEGylated lipid in the membrane, the PEG-rich aqueous phase initially occupied the outer position, contacting the membrane, and fully surrounded the dextran-rich aqueous phase (Scheme 1). This is reasonable since incorporation of PEGylated lipid in the membrane should favor interactions with the PEG-rich phase over the dextran-rich phase. Upon exposure to the 2× hypertonic sucrose solution, GVs with PEGylated membranes formed predominantly budded structures (Scheme 1, **B**) similar to those shown in Figures 2−4 regardless of the encapsulated ATPS composition.

In contrast, when DOPGs (and no PEGylated lipids) were incorporated in the membranes, we saw different results depending on the ATPS (Table 1 and Scheme 2). In isotonic solution, the ATPS with PEG 4.6 or 8 kDa and dextran 10 kDa had the dextran-rich phase contacting the membrane; however those with dextran 70 or 500 kDa had the PEG-rich phase contacting the membrane. Differences in phase position can be thought of in terms of the relative magnitudes of the interfacial tensions at three boundaries within the ATPS GVs: (i) the aqueous−aqueous interface, (ii) the PEG-rich phase (PP)−membrane interface, and (iii) the dextran-rich phase (DP)−membrane interface. The interfacial tension at the aqueous−aqueous interface depends on ATPS composition (polymer MW and weight percent) and can be experimentally determined for bulk solutions via spinning drop tensiometry.[48−50] ATPS prepared with PEG 4.6 or 8 kDa and dextran 10 kDa had a bulk interfacial tension 10× higher than that for ATPS with PEG 8 kDa and the larger dextrans, 70 or 500 kDa. Within GVs the tension at the aqueous−aqueous interface may be lower due to <100% encapsulation of either of the two phase-forming polymers.[39,51]

The magnitude of the interfacial tensions between the phases and the lipid bilayer should vary with lipid chemistry but is not readily measured. It is perhaps reasonable to assume that the relative ordering of PP−lipid vs DP−lipid interaction potentials is the same for the different ATPS compositions. However, based on the bulk ATPS interfacial tensions, it is possible that both aqueous phase−membrane interfacial tensions may be higher for the ATPS with smaller dextrans. All four ATPSs have on average smaller volume of DP than PP in the bulk. Therefore, if the DP−PP interfacial tension was the primary determinant of relative phase position, DP should be the inner phase, as this minimizes the ATPS interfacial area. However, DP was the inner phase only for the higher MW dextran ATPS compositions, indicating the importance of differences in the PP−lipid vs DP−lipid interfacial tensions. GVs prepared without PEGylated lipid did not bud upon exposure to 2× hypertonic sucrose solutions at room temperature, with the exception of the PEG 8 kDa/dextran 70 kDa ATPS (Scheme 2B, C). Interestingly, the 500 kDa dextran ATPS GVs, which have the PP as the exterior phase under isotonic conditions, reversed relative phase positions such that DP was in contact with the membrane when dehydrated (Scheme 2C). Thus, for the non-PEGylated membranes, the interior DP was observed *only* for the lower DP−PP interfacial tension ATPS compositions, suggesting that increased polymer concentrations may impact the interaction between the DP and/or PP with the membrane more so than with each other.

Conclusions

Giant lipid vesicles filled with a PEG/dextran aqueous two-phase system respond to increased external osmotic pressure by shrinking and, when membrane elasticity permits, forming budded morphologies in which one or more spherical buds extends from the "parent" vesicle. Buds contain a different aqueous phase from the main body of the vesicle. Partitioning of solutes such as proteins within the encapsulated aqueous phase system results in asymmetric distributions of these solutes upon budding. Improved partitioning is also observed, due to the increased polymer concentrations that result from hyperosmotic stress. The structural and (bio)chemical polarity induced by budding can be reversed by placing the ATPS-containing GVs into a lower osmolarity solution, whereupon they revert to a spherical shape. The propensity to form buds depends strongly on lipid composition, with increased percentages of budded structures with increasing PEGylated lipid mole fraction up to the mushroom-to-brush transition, after which the percent budded vesicles remains essentially constant. The compositions of both the lipid membrane and the polymer solution impact the observed structures, with the ATPS composition dominating for DOPC/DOPG membranes. The GV osmotic pressure-induced budding studies presented here differ substantially from previous reports in both the presence of the ATPS and the absence of micron-scale lipid phase domains in the GV membrane.

Although the mechanism via which initial polarity is generated in this simple model system is different from any postulated for living cells, asymmetric protein microcompartmentation within these structures is interesting as an experimental model system for investigating the *effects* of biochemical polarity in cell-scale structures. The onset and maintenance of biochemical polarity in living cells is critical not only in the development and morphogenesis of higher organisms but also in numerous single-celled organisms such as the bacterium *Caulobacter*

(51) Sun, B.; Chiu, D. *Anal. Chem.* **2005**, *77*, 2770−2776.

crescentus. Much emphasis has been placed on identifying genes and proteins involved in polarity. These important genetic studies should be combined with investigations of more general cytoplasmic mechanisms for building on an asymmetry in one cellular component to generate the degree of polarity achieved, e.g., in dividing *Caulobacter*, which forms two nonidentical daughter cells, one of which is motile while the other is not.[52] The importance of whole-cell mechanisms beyond the role(s) of individual proteins has been recognized;[53] the asymmetrically compartmentalized model cells described here could serve as an experimental model system to explore such routes to complex, functional biochemical polarity starting from initially simple chemical polarity. We note that, in living cells, asymmetry is observed not only in the distribution of cytoplasmic proteins but also in the cell membrane itself. Control over the spatial distribution of molecules within our model cytoplasm could provide a mechanism for modeling polarity in the lipid membranes as well; investigations in this direction are underway.

Acknowledgment. We thank the National Science Foundation (CHE-0239629) and Pennsylvania State University for financial support of this work. C.D.K. also acknowledges support from a Beckman Young Investigator Award, a Sloan Fellowship, and a Camille Dreyfus Teacher-Scholar Award. A.-S.C. acknowledges support from the Knut and Alice Wallenberg Foundation. Confocal microscopy images were obtained at the Center for Quantitative Cell Analysis, a shared facility of The Huck Institutes of the Life Sciences at The Pennsylvania State University.

Supporting Information Available: Experimental methods, ATPS osmolality as a function of polymer weight percent composition, optical microscope images of reversible ATPS GV budding, and graphs of polymer and protein partitioning within bulk ATPS and ATPS GVs as a function of osmolality. This material is available free of charge via the Internet at http://pubs.acs.org.

JA077439C

(52) Viollier, P. H.; Shapiro, L. *Curr. Opin. Microbiol.* **2004**, *7*, 572−578.
(53) Harold, F. M. *Microbiol. Mol. Biol. Rev.* **2005**, *69*, 544−564.